P7.10 EYEWALL EVOLUTION OF HURRICANE KATRINA NEAR LANDFALL USING NEXTRAD REFLECTIVITY AND RADIAL VELOCITY DATA

Kimberly D. Campo and Thomas M. Rickenbach

Department of Meteorology, San Jose State University

1. Introduction[1]

Katrina was an exceptionally large and intense hurricane causing an estimated $75 billion in damage and 1,336 deaths across five states. The sheer physical size of Katrina caused devastation far from the eye, with an estimated radius of maximum winds extending nearly 56 km, making Katrina quite possibly the largest hurricane of its strength on record. On 29 August, Katrina's storm surge breached the levee system that protected New Orleans, flooding nearly 80% of the city and permanently destroying 275,000 to 300,000 homes. The extent, magnitude, and impacts of the damages caused by Katrina are astounding, resulting in public outrage in the U.S. government's response to the disaster, and a realization that further studies are vital to better understand landfalling Gulf Coast hurricanes.

Since the late 1960s, numerous studies have been conducted to better understand the rapid intensification (RI) a tropical cyclone (TC) undergoes over the open ocean. While forecasting TC intensity changes prior to landfall is imperative, understanding the structure and decay patterns of TCs post-landfall and when the TC is only a few hundred kilometers off the coast, is crucial since populations continue to increase in these vulnerable coastal regions.

TCs are driven by latent heat flux over the warm ocean surface. This heat flux increases rapidly with increasing wind speed, making mature TCs effective heat engines. Upon landfall, this latent heat flux shuts down and frictional dissipation decreases the storm's kinetic energy, causing the storm to dissipate and the eye to fill with clouds and precipitation.

This study aims to document the decay patterns of Hurricane Katrina as it made landfall along the Gulf Coast using land-based NEXRAD radar reflectivity and radial velocity data. Section 2 provides a literary background of previous landfalling TC studies, followed by a synoptic summary of Katrina and a discussion of RI periods in section 3. The WSR-88D radar and NCAR Solo 5 provides details of the results found in the examination of the evolution of the eyewall region of Hurricane Katrina as the system approached and made landfall, followed by concluding remarks in section 6.

[1] *Corresponding Author Address:* Kimberly Campo, Department of Meteorology, San Jose State University, One Washington Square, San Jose, CA 95192

2. Background and previous studies

One of the main goals of NOAA's Hurricane Research Division (HRD) is to augment the ability to predict TC intensity upon landfall. A TC undergoes large intensity changes as it approaches land, but little is understood in regards to mechanisms for these intensity changes. Accurate TC wind field derivations and surface measurements near and post-landfall are essential to understanding landfalling TC decay. In addition, the United States Weather Research Program (USWRP) Fifth Prospectus Development Team (PDT-5) identified six key research objectives to better understand and forecast landfalling TCs (Marks et al. 1998), one of which is to research and develop techniques to improve wind field and precipitation patterns of landfalling systems.

A major source of difficulty in predicting hurricane intensity, wind fields, and storm surge at landfall in the past have been the inability to measure the surface wind field directly and to predict how the system changes in response to both external and internal forcing (Marks et al. 1998). Currently, surface wind field parameters are estimated using flight-level wind observations conducted by both NOAA's HRD and air force reconnaissance (AFRES) aircraft. These flight-level observations are adjusted to estimate surface wind speeds, using a planetary boundary layer (PBL) model (Zhang et al. 1999). Multiple flight-level research experiments and Doppler radar measurements suggest that maximum mean wind speeds are found at 0.5-2.0 km above sea level, while HRD flights are conducted at 2.5-3.2 km levels. This method of estimating the surface wind field is problematic due to variations with height of the storms' structure, environmental wind shear, and our uncertainty involving the internal dynamics of TCs.

Since 1982, NOAA's HRD has conducted a series of experiments with research aircraft

using multiple Global Positioning System (GPS) dropwindsondes which measure the vertical profiles of wind, temperature, and humidity from flight level to the surface. Dropwindsondes provide the high-quality data source needed for the improvement of TC winds and thermodynamic analysis. These data have reduced 12-60h model forecast track errors by as much as 30% (Marks et al. 1998). Franklin et al. (1999) estimated the quantitative relationship between flight-level and surface winds by analyzing GPS dropwindsonde data. Their results suggest that to reasonably assess the surface wind field, the aircraft would have to fly at the 800-1200 m level.

The next goal the PDT-5 intends to accomplish is the improvement of forecasting the near surface wind field during landfall (6 hours before and after landfall), pre-landfall (the period up to 48h prior to landfall), and post-landfall (>6h after landfall). To complete this task, a mobile observing system was developed which is based upon the NOAA (WP-3D and G-IV), NASA, and AFRES aircraft, portable profiles, Doppler radars, and surface mesonets. This mobile unit is placed in the landfalling path of an approaching TC, providing a unique opportunity to sample the destructive winds of a TC offshore before and during landfall.

Although the advent of new technological tools used to better understand and predict landfalling TC wind fields and decay patterns has proved promising to our understanding of landfalling TCs, the continued use of classical methods of observing TC changes remains vital. The land-based Weather Surveillance Radar-1998 Doppler (WSR-88D) has been used to verify the new observing systems (e.g., Geerts et al. 2000, Dodge et al. 1999). WSR-88D units routinely scan regions out to ~400 km range every 6 minutes, thus have been used to monitor TCs that track near populated coastlines. Lee and Marks (2000) and Lee et al. (2000) demonstrated that TC wind fields could be retrieved using the ground-based velocity track display (GBVTD) method. Although errors do exist, algorithm improvements of WSR-88D velocity interpretation are continuously in development (Harasti et al. 2004). Harasti et al. (2004) showed that GBVTD and tracking radar echoes by correlation (TREC) wind estimates using improved WSR-88D algorithms have the ability to retrieve TC wind speeds with an accuracy of ~2 m s^{-1} or better. To skillfully forecast TC surface wind fields, observations, theory, and modeling must continually be improved.

Powell and Houston (1998) combined automated surface observations (ASOS) and flight-level Air Force reconnaissance aircraft data, assimilated into a PLB model, to describe changes in the surface wind field of several landfalling hurricanes. Dodge et al. (1999) used the pseudo-dual Doppler radar on HRD's WP-3D aircraft to derive the wind field of Hurricane Danny as it made landfall along the Gulf Coast, and included NEXRAD radial velocities in their synthesis for comparison. Geerts et al. (2000) used ground-based radar, EDOP, and ER-2 passive microwave imagery to observe the changing surface wind field of Hurricane Georges as it made landfall in the Dominican Republic.

By using a combination of WSR-88D land-based Doppler velocities with the damage track of Hurricane Andrew, Wakimoto and Black (1994) were able to identify important information regarding the structural changes that occurred as Andrew made landfall. Tuttle and Gall (1999) found it useful to complement single-Doppler velocities with estimates of the horizontal winds of landfalling hurricanes, by objectively tracking reflectivity echo patterns as they rotate about the eye. This method was found to work reasonably well for well organized hurricanes, but not in the case of Katrina whose eye became significantly asymmetrical near landfall with the deterioration of the eyewall in the southwest quadrant.

3. Storm synoptic history

a. Synoptic history

On 23 August 2005 the National Hurricane Center (NHC) reported that Tropical Depression Twelve had formed over the southeastern Bahamas, upgrading to Tropical Storm Katrina on the morning of 24 August. The storm continued to intensify along its slow northwesterly then westerly track through the Bahamas. By landfall in south Florida, at 1030 UTC on 25 August, Katrina had strengthened to a Category 1 Hurricane. Katrina spent only seven hours over land before it entered the warm waters of the Gulf of Mexico (GOM) along a nearly due westward path. Due to the unusually warm upper ocean thermal structure of the GOM (referred to in detail in section 3b) Katrina quickly regained hurricane strength with maximum sustained winds of 65 kts at 0600 UTC on 26 August (Knabb et. al 2005). A strong, very large, upper-level ridge dominated the entire GOM 26 August, resulting in a region of weak wind shear and efficient upper-level divergence (two key ingredients for hurricane development).

These synoptic conditions, along with the thermal structure of the GOM, allowed Katrina to embark upon two periods of rapid intensification (RI) (defined by a 30 kt or greater intensity increase within a 24-h period) between 26 and 28 August. The first period of RI involved an increase in maximum sustained winds from 65 kts to 100 kts by 1200 UTC on 27 August (Knabb et. al 2005). During the remainder of the day, Katrina nearly doubled in size after undergoing one of two concentric eyewall cycles (Willoughby et al 1982) in which the inner eyewall deteriorated being replaced by a new, outer eyewall.

The strong upper-level ridge that had kept Katrina on its westward path, weakened and shifted eastward toward Florida, while a mid-latitude trough amplified over the north-central United States (Knabb et. al 2005). This pattern caused Katrina to gradually shift toward the northwest on 28 August, followed by a second, more intense RI. Katrina strengthened from a low-end Category 3 hurricane to a Category 5 with maximum sustained winds of 145 kt by 1200 UTC 28 August after undergoing a second concentric eyewall cycle. At 1800 UTC, Katrina reached its peak intensity of 150 kt 170 n mi southeast of the Mississippi River with hurricane-force winds extending 90 n mi from the storm's center (Knabb et. al, 2005). Katrina was not only an incredibly intense hurricane, but also an exceptionally large one. As the upper-level ridge continued to move eastward, the mid-latitude trough that followed forced Katrina to track nearly due north toward the northern Gulf coast.

Katrina rapidly weakened as it approached the Louisiana/Mississippi coast primarily due to internal structural changes within the storm, specifically the deterioration of the inner eyewall in the southwest quadrant (Fig. 1a). This rapid weakening could have also been aided by increasing wind shear associated with the oncoming trough, and entrainment of dry air that was observed eroding the convection on the western side (Knabb et. al 2005). The weakening of major hurricanes as they approach the northern Gulf coast has been observed on several occasions and detailed studies of such cases can be found on the NHC website. Nonetheless, Katrina made landfall as a strong Category 3 hurricane at 1110 UTC 29 August near Buras, Louisiana with estimated maximum sustained winds of 110 kt. Two hours later, Katrina made its final landfall near the Louisiana/Mississippi boarder with hurricane force winds extending outward 190 km.

The eyewall quickly filled in as Katrina moved inland and the storm's overall intensity decayed rapidly, losing hurricane-strength 160 km inland, near Jackson, Mississippi by 0000 UTC 30 August. Katrina accelerated as it merged with an eastward-moving trough over the Great Lakes, affecting the central U.S. and southern Quebec as it moved north.

b. GOM Thermal Structure 29 August

A weekly GOM surface dynamics report issued the week of 29 August by NOAA/AMOL, reveals the complex thermal structure of the GOM throughout the duration of Katrina. The report overlays Katrina's track with graphics of: sea height anomalies (SHA); Tropical Cyclone Heat Potential (TCHP); satellite-derived sea surface temperatures (SST); altimetry-derived 26° isotherm; and the warm anticyclonic features of the Loop Current (LC)[1].

Katrina underwent two periods of RI after traveling over a number of such warm features in the GOM. Satellite-derived SST fields exhibit high values, warmer than 29°C, over most of the GOM with the depth of the 26°C isotherm in direct correlation. It has been shown (Gray 1968) that there exists a strong relationship between the depth of the 26°C isotherm and tropical cyclogenesis. For this reason TCHP was introduced to quantify the amount of heat stored in the upper ocean.

Katrina crossed both the LC and R05-1, a warm anticyclonic ring that dominates the surface dynamics of the eastern GOM, prior to its final RI period early on 28 August. Altimetry-derived TCHP values in the GOM average 90 kJ cm^{-2} within the LC, 70 kJ cm^{-2} over the eastern GOM, and up to 120 kJ cm^{-2} in the center of R05-1. It is likely that these abnormally warm features within the GOM region contributed significantly to Katrina's intensification from a low end Category 1 hurricane on 26 August, to a strong Category 5 on 28 August.

4. Data and analysis

a. WSR-88D data and analysis

[1] For more information about these products refer to www.amol.noaa.gov/phod/cyclone/data/

The National Weather Service (NWS) WSR-88D at New Orleans, Louisiana (hereafter referred to as KLIX) operates in a volume-scan mode with 6-min intervals between scans, a frequency of 2700 to 3000 MHz, and a wavelength of 10-11 cm. WSR-88D radars provide Doppler information under high pulse repetition frequencies (PRF) with ranges of about 150 km, and reflectivity data only in the low PRF mode out to about 430 km range. The KLIX NWS office is located in Slidell, Louisiana with a station elevation of 8 m and radar tower height of 30 m.

In the present study, WSR-88D archive level II digital data were analyzed using NCAR's SOLO software. The archived level II data are analyzed in 5-10 min intervals for he 3-h prior to landfall, at 1310 UTC 29 August, and up to 1-h post landfall. Only data 3-h prior to landfall were used due to the range of WSR-88D's base reflectivity (230-km range, 0.5° elevation). This data was compared to NHC VORTEX data, reported at similar time intervals, to give confidence to the radar measurements (VORTEX reports used can be found in appendix A).

The KLIX WSR-88D provided near-surface reflectivity and Doppler radial winds in Katrina's core. To facilitate evaluation of the storm's structural evolution, radial snapshots of inbound and outbound base velocities were generated (using Solo) that closely represent the horizontal wind structure on each side of the hurricane (Fig. 1b), and clearly indicate rotation about the eye. The nyquist velocity (defined as the maximum unambiguous velocity that can be detected at a given PRF was measured in each individual snapshot using Solo's data widget option. PRFs ranged from 833 to 1100 Hz depending on the pulse range used during the analysis, and nyquist velocities were 27.5 m s^{-1} and 22 m s^{-1} respectively.

Doppler radial velocities are compared between the northeast eyewall and the southwest eyewall of Katrina to estimate the translational speed of the system as it approached the Northern Gulf Coast. This was done by taking the difference between the maximum radial velocity values of the eastern and western eyewall region, assuming the difference was entirely due to the translational motion of the hurricane. This is hereafter referred to as the "difference method" of storm motion. This estimate of the translational speed was then compared to the speed of hurricane motion obtained by tracking the storm's center of circulation prior to and during landfall. This is hereafter referred to as the "tracking method" of storm motion. The assumption was that any difference in storm motion between these two methods was due to internal fluctuations within the eyewall. Observations further suggest a significant decrease in the translational speed of Katrina's eye as the storm approached land, as well as a significant decay of maximum surface wind speeds as the system progressed inland. An observed slight increase in maximum surface wind speeds moments after landfall, suggests that the eastward moving mid-latitude trough had immediate impacts on Katrina at landfall. Section 5 provides details of the results found in the examination of the evolution of the eyewall region of Hurricane Katrina as the system approached and made landfall.

b. Adequacies and inadequacies of using Doppler data

Coastal radars can provide valuable information in landfalling storms, such as accurate storm positioning, which is also useful to estimate hurricane speed of motion if the eye is nearly symmetrical. By tracking the center of circulation within the eyewall through successive images, the motion of the hurricane can be calculated directly. However, if the eyewall is asymmetrical, as in the case of Katrina, locating the center of circulation can be quite difficult and result in considerable errors.

Ground-based Doppler wind estimates are possible only <100 km from the radar site and radar base beam elevations at 100-km distance exceed 1500 m. Thus, shorter ranges (<60 km) are required to observe detailed and accurate near-surface eyewall structure of a hurricane. 1015 UTC, one hour prior to initial landfall along the northern Gulf Coast, the center of Katrina was 150 km from the KLIX radar, but was much too distant for the radar to provide concurrent near-surface wind estimates close to the eye. Not until two hours later did Katrina's eye come within measurable distance from the radar to provide accurate surface wind estimates.

5. Results

We begin by first presenting the general structural features of Hurricane Katrina as it approached the northern Gulf Coast. TRMM 85 GHz imagery at 2133 UTC 28 August revealed a developing outer eyewall, with subsequent microwave scans depicting the inner eyewall

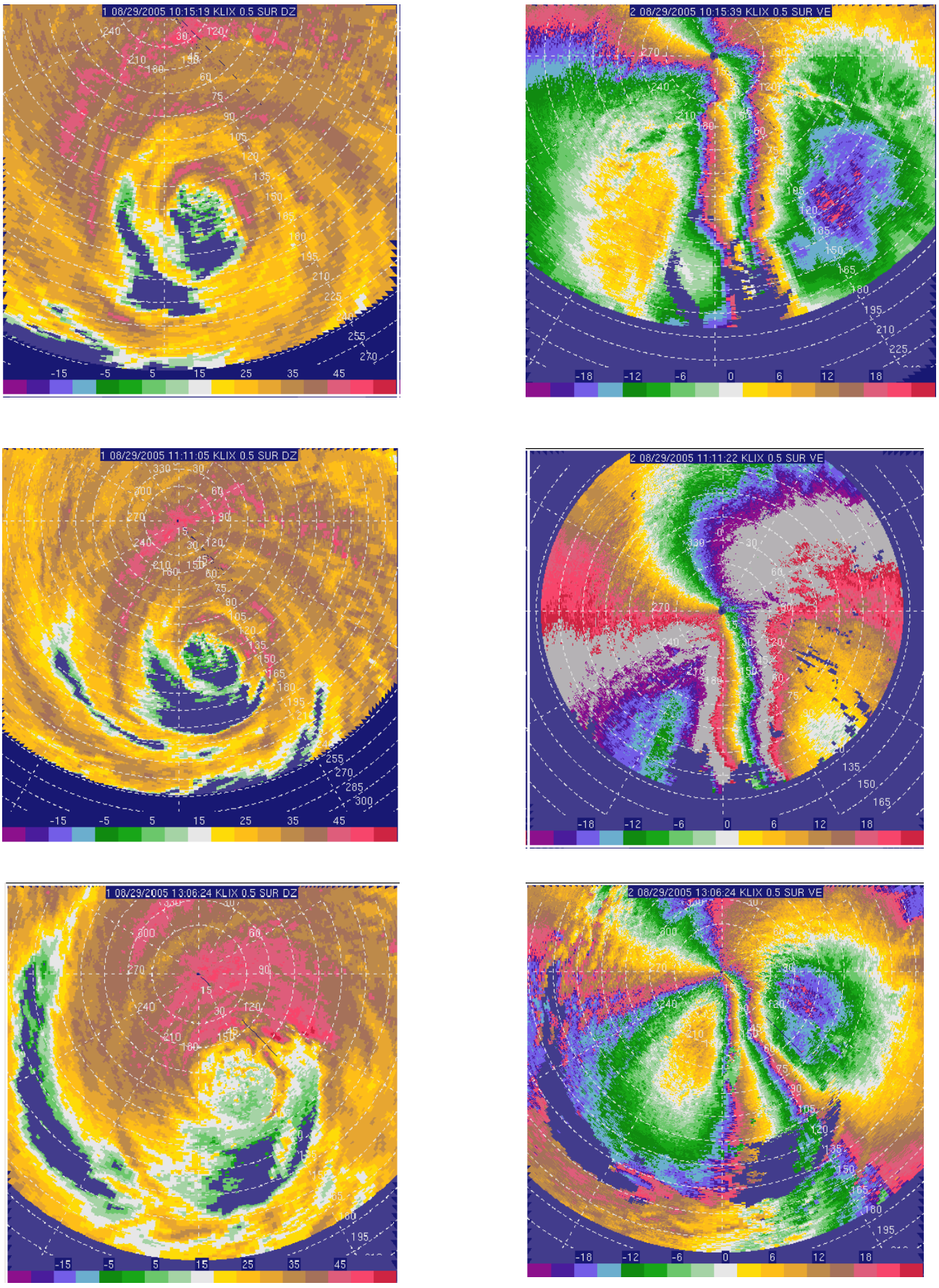

FIG. 1. Base reflectivity (left column) and radial velocity (right column) of Hurricane Katrina from the KLIX WSR-88D at (a, b) 1015 UTC 29 August, (c, d) 1111 UTC 29 August, and (e, f) 1306 UTC 29 August. Reflectivity is measured in dBZ and velocity in m s^{-1} .

steadily eroding, especially on the southwest side (Knabb et. al 2005). By 1015 UTC, the eyewall contraction had completed, resulting in an asymmetrical eyewall shape and a significant deterioration of the eyewall on the southwest side, as seen in Fig. 1. Strong winds extend far to the north and east of the center, but weakened rapidly with radial distance on the south and west sides. This asymmetry was consistent with the storm motion of 7-10 ms^{-1} toward the northeast.

WSR-88D base velocity analysis reveals that Katrina strengthened slightly prior to initial landfall (while over the warm GOM waters) as the newly formed eyewall adjusted and attempted to reorganize.

a. Comparison of WSR-88D base velocities to maximum flight-level winds

Flight-level winds are compared to WSR-88D base velocities to validate the accuracy of our radar measurements. Initially the two compare reasonably well due to the analogous altitude at which both methods are sampling. However, as Katrina approached the coastline and came within measurable distance from the radar, the difference between the sampling levels are much too large for accurate comparison.

At 1015 UTC, Katrina was 150 km from the KLIX radar with maximum base velocity measurements of 71 m s^{-1} in the northeast quadrant at a height of 2200 m (see Table 1). Maximum 700 mb (2400 m) flight-level winds confirm the strength of these winds with a measurement of 130 kt (67 m s^{-1}) northeast of the eye at around this time. It is surprising that the two measurements compare so well because maximum flight-level winds are sampled from a single point, while the radar, at this distance, is sampling a very large volume and taking the average of the velocities within that volume.

b. Structural changes before and after landfall

Base velocities show wind speeds, both to the east and west of the eye, continued to increase until initial landfall, helping to maintain the asymmetrical distribution of winds near the core. The strongest winds prior to landfall occurred around 1040 UTC 29 August, with base velocity measurements of 72.5 m s^{-1} northeast of the eye and 57 m s^{-1} to the southwest. A large difference in storm motion between the difference method versus tracking method is evident during this time (Fig. 2). We interpret this difference to substantial asymmetry within the eyewall region.

After landfall, at 1110 UTC, wind speeds decreased significantly, especially to the east of the eye. WSR-88D base velocity measurements of 71 m s^{-1} in the northeast quadrant, and 55 m s^{-1} in the southwest quadrant were observed at landfall, with the center of Katrina still 120 km from the radar and base beam elevations at 1700 m. Flight-level (2400 m) winds remain comparable at this distance with maximum flight-level winds of 124 kt in the southeast quadrant. In the hours prior to final landfall, wind speeds continued to decrease to the northeast of the eye, while winds increased slightly to the south (Fig. 3). This trend led to decrease the asymmetrical wind structure about the eye.

TABLE 1. Listing of NEXRAD maximum base velocity measurements (ms^{-1}) in both the northeast (NE) and southwest (SW) quadrants. Distance is the approximate distance of Katrina's center from the KLIX radar site in km and height is the base beam elevation at the 0.5° elevation angle at that distance.

Time	NE	SW	distance (km)	height (km)
1015	70.5	56.5	147.43	2.2
1028	71.5	55.5	142.43	1.9
1039	72.5	55	136.14	1.7
1049	72	57	131	1.7
1055	72	56	128.04	1.7
1105	71	56.5	122.81	1.7
1111	71	55	119.81	1.6
1122	70	56	114.27	1.6
1133	70.5	57	108.32	1.5
1138	70.5	57	105.5	1.4
1149	70	59	99.21	1.3
1200	69	59	94.4	1.2
1217	69	59	87.1	1.1
1227	69	58	82.6	1
1238	69	58.5	76.5	0.9
1249	67.5	58	70.67	0.9
1255	67.5	58	68.1	0.8
1306	68	57	63.8	0.8
1316	68.5	56	59.4	0.6
1327	68.5	53.5	52.93	
1338	67	52	47.9	
1344	67	52.5	45.4	
1349	66	55	43.4	
1354	64.5	55	41.56	
1400	62.5	54	39.5	

Figure 4 shows the general decreasing trend in the translational speed of Katrina after landfall. During this period, from 1100-1400 UTC, Katrina's eye began to fill rapidly as the eyewall strength and structure decayed. An interesting feature occurred at 1230 UTC in which a slight increase in hurricane speed using both the difference and tracking methods is observed. The cause of this feature is uncertain, but we speculate it may be due to a brief respite in frictional dissipation as the eyewall region passed over Lake Pontchartrain.

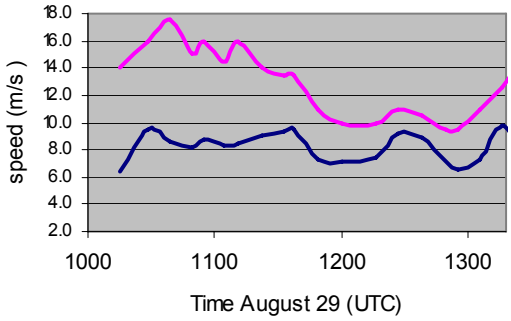

FIG. 2. A time series comparing the difference method (pink) of estimating the translational speed to the tracking method (blue) of Hurricane Katrina.

By 1150 UTC, the difference in storm speed from the difference vs. tracking methods decreased significantly. This observation may be a result of eyewall structure becoming more symmetrical as Katrina weakened and the eye began to fill (Fig. 2). Theoretically, the difference between the, difference vs. tracking methods equates to an estimate of the internal structural variations within the eye. However, in this case, accurate and reliable surface wind measurements were not available, and because Katrina was much too far from the radar to provide surface wind estimates before 1250 UTC 29 August, it is difficult to infer how much of the variation seen in Fig. 2 is due to internal eyewall fluctuation. The increase in storm speed from both methods seen in Fig. 2 at 1300 UTC, just before final landfall, is likely due to acceleration of Katrina merging with the eastward moving trough.

Base velocities at final landfall, 1310 UTC, were 68.5 m s^{-1} in the northeast quadrant and 56 m s^{-1} in the southwest quadrant with Katrina within measurable range (60 km) of the radar. At this range base velocities should provide accurate near-surface wind estimates, and do compare reasonably well with NHC's initial best track intensity of 120 kt. Blackwell (2000) stated that nearby Doppler radars may provide better estimates of maximum winds if base velocities are sampled below aircraft flight level, but there is no guarantee that WSR-88D velocities correspond to maximum tangential winds. Stronger winds could be at lower altitudes or may not be oriented along the radar beam (Blackwell, 2000). However, because Katrina tracked nearly due north, almost directly toward the KLIX radar, WSR-88D velocities should reflect near-surface winds.

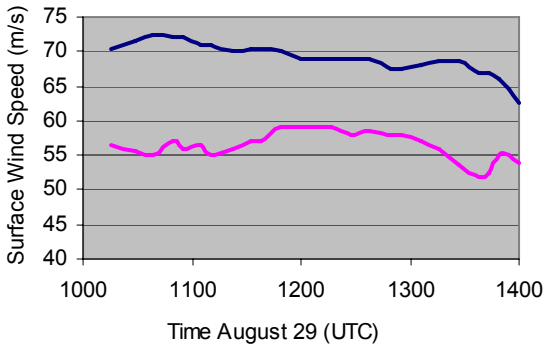

FIG. 3. Time series of maximum surface wind speeds 29 August. Blue line represents wind in the northeast quadrant and pink represents the southwest quadrant.

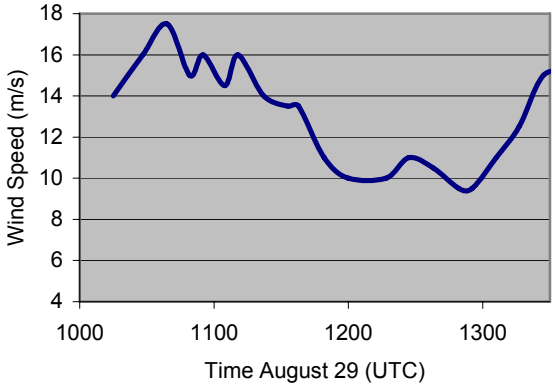

FIG. 4. A time series of Hurricane Katrina's translational speed using the difference method from 1000-1330 UTC 29 August.

It is worth noting that Katrina's landfall intensity remains under great debate. Analysis of several dropwindsonde profiles from 29 August suggests maximum surface winds were likely 103 kt or higher, while the Stepped Frequency Microwave Radiometer (SFMR) aboard the Hurricane Hunter WP-3D aircraft measured 99 kt

(Knabb et. al 2005). The best track intensity of Katrina has also been adjusted downward to 110 kt at final landfall due to post-storm analysis, making the central pressure of 920 mb the lowest on record in the Atlantic basin for an intensity of 110 kt (Knabb et. al 2005).

6. CONCLUTIONS

The evolution of the eyewall region of Hurricane Katrina was examined as it made landfall along the Gulf coast on 29 August 2005, using KLIX NEXRAD reflectivity and radial velocity data. It was shown that Katrina had decayed rapidly as the system approached the Coast, primarily due to the erosion of the eyewall on the southern side.

After initial landfall, at 1110 UTC 29 August, Katrina's near-surface wind speeds decreased significantly, especially to the east of the eye, inducing a more symmetrical distribution of wind speeds about the eye. A time series comparison (Fig. 2) of the difference method of estimating hurricane translational speed, to the tracking method, revealed the internal structural variations within the eye after landfall. The eyewall quickly filled in as Katrina moved inland and the storm's overall intensity decayed rapidly.

NEXRAD analysis reveals that Katrina may have had slightly stronger winds at landfall than those reported, 68.5 m s^{-1} as opposed to 62 m s^{-1} reported from the HRD. The uncertainty of Katrina's maximum surface wind speeds at landfall indicates that further research, and the development techniques to improve boundry layer wind maxima of landfalling systems, is warranted.

7. APPENDIX

HRD VORTEX Data:

http://euler.atmos.colostate.edu/~vigh/recon/

URNT12 KNHC 291015
VORTEX DATA MESSAGE
A. 29/10:02:00Z
B. 28 deg 59 min N
089 deg 36 min W
C. 700 mb 2381 m
D. NA kt
E. NA deg nm
F. 098 deg 109 kt
G. 349 deg 035 nm
H. 918 mb
I. 11 C/ 3047 m
J. 18 C/ 3050 m
K. 15 C/ NA
L. CLOSED
M. C25
N. 12345/ 7
O. 0.02 / 1 nm
P. AF306 2112A KATRINA OB 08
MAX FL WIND 128 KT NE QUAD 08:57:50 Z

URNT12 KNHC 291113
VORTEX DATA MESSAGE
A. 29/10:55:10Z
B. 29 deg 11 min N
089 deg 37 min W
C. 700 mb 2411 m
D. NA kt
E. NA deg nm
F. 006 deg 088 kt
G. 261 deg 040 nm
H. 925 mb
I. 11 C/ 3050 m
J. 18 C/ 3049 m
K. 17 C/ NA
L. CLOSED WALL
M. C22
N. 12345/ 7
O. 0.02 / 1 nm
P. AF300 2212A KATRINA OB 03
MAX FL WIND 88 KT W QUAD 10:43:30 Z

URNT12 KNHC 291113 CCA
VORTEX DATA MESSAGE
A. 29/10:55:10Z
B. 29 deg 11 min N
089 deg 37 min W
C. 700 mb 2411 m
D. NA kt
F. 006 deg 088 kt
G. 261 deg 040 nm
H. 920 mb
I. 11 C/ 3050 m
J. 18 C/ 3049 m
K. 17 C/ NA
L. CLOSED WALL
M. C22
N. 12345/ 7
O. 0.02 / 1 nm
P. AF300 2212A KATRINA OB 03 CCA
MAX FL WIND 88 KT W QUAD 10:43:30 Z

URNT12 KNHC 291142
VORTEX DATA MESSAGE
A. 29/11:32:30Z
B. 29 deg 21 min N
089 deg 35 min W
C. 700 mb 2413 m
D. NA kt
E. NA deg nm
F. 139 deg 127 kt
G. 051 deg 036 nm
H. 921 mb
I. 9 C/ 3043 m
J. 17 C/ 3045 m

K. 16 C/ NA
L. CLOSED
M. C25
N. 12345/ 7
O. 0.02 / 2 nm
P. AF306 2112A KATRINA   OB 14
MAX FL WIND 134 KT E QUAD 10:13:20 Z
EYEWALL STRUCTURE WEAKENING IN SOUTH

URNT12 KNHC 291228
VORTEX DATA MESSAGE
A. 29/12:09:50Z
B. 29 deg 33 min N
  089 deg 34 min W
C. 700 mb 2420 m
D. NA kt
E. NA deg   nm
F. 123 deg 116 kt
G. 34 deg 034 nm
H.   923 mb
I. 10 C/ 3049 m
J. 18 C/ 3053 m
K. 16 C/ NA
L. CLOSED WALL
M. C23
N. 12345/ 7
O. 0.03 / 1 nm
P. AF300 2212A KATRINA   OB 10
MAX FL WIND 124 KT SE QUAD 11:07:50 Z
SFC CENTER W/IN 5NM OF FL CENTER
EYE WALL WEAKER TO SOUTH
MAX FL TEMP 19C 270 / 10 NM FROM FL CNTR

URNT12 KNHC 291258
VORTEX DATA MESSAGE
A. 29/12:47:20Z
B. 29 deg 41 min N
  089 deg 36 min W
C. NA mb NA   m
D. NA kt
E. NA deg   nm
F. 136 deg 117 kt
G. 050 deg 058 nm
H.   923 mb
I. 12 C/ 2447 m
J. 20 C/ 2440 m
K. 18 C/ NA
L. OPEN SE
M. C30
N. 12345/NA
O. 0.02 / 1 nm
P. AF306 2112A KATRINA   OB 19
MAX FL WIND 129 KT E QUAD 11:45:10 Z

URNT12 KNHC 291342
VORTEX DATA MESSAGE
A. 29/13:23:10Z
B. 29 deg 50 min N
  089 deg 37 min W
C. 700 mb 2455 m
D. NA kt
E. NA deg   nm
F. 324 deg 085 kt
G. 226 deg 018 nm
H.   925 mb
I. 14 C/ 3052 m
J. 18 C/ 3048 m
K. 16 C/ NA
L. OPEN SE
M. C30
N. 12345/ 7
O. 0.02 / 1 nm
P. AF300 2212A KATRINA   OB 18
MAX FL WIND 124 KT SE QUAD 11:07:50 Z
EYE RAGGED

URNT12 KNHC 291402
VORTEX DATA MESSAGE
A. 29/13:54:20Z
B. 29 deg 58 min N
  089 deg 37 min W
C. NA mb NA   m
D. NA kt
E. NA deg   nm
F. 164 deg 121 kt
G. 085 deg 026 nm
H.   926 mb
I. 14 C/ 2439 m
J. 20 C/ 2442 m
K. 18 C/ NA
L. OPEN SW
M. E180/35/25
N. 12345/NA
O. 0.02 / 1 nm
P. AF306 2112A KATRINA   OB 25
MAX FL WIND 121 KT E QUAD 13:46:50 Z

URNT12 KNHC 291454
VORTEX DATA MESSAGE
A. 29/14:29:30Z
B. 30 deg 07 min N
  089 deg 37 min W
C. 700 mb 2461 m
D. NA kt
E. NA deg   nm
F. 157 deg 126 kt
G. 73 deg 027 nm
H.   927 mb
I. 11 C/ 3042 m
J. 17 C/ 3049 m
K. 16 C/ NA
L. OPEN SW
M. E06/30/24
N. 12345/ 7
O. 0.02 / 1 nm
P. AF300 2212A KATRINA   OB 22
MAX FL WIND 128 KT E QUAD 13:33:50 Z
EYE RAGGED

URNT12 KNHC 291500
VORTEX DATA MESSAGE
A. 29/14:42:40Z
B. 30 deg 11 min N
  089 deg 36 min W

C. NA mb NA m
D. NA kt
E. NA deg nm
F. 179 deg 120 kt
G. 097 deg 019 nm
H. 928 mb
I. 18 C/ 2435 m
J. 19 C/ 2435 m
K. 19 C/ NA
L. OPEN SW
M. E210/35/25
N. 12345/NA
O. 0.12 / 2 nm
P. AF306 2112A KATRINA OB 30
MAX FL WIND 120 KT E QUAD 14:36:40 Z
MAX FL TEMP 20 C, 99 / 13NM

URNT12 KNHC 291527
VORTEX DATA MESSAGE
A. 29/15:16:50Z
B. 30 deg 19 min N
089 deg 38 min W
C. 700 mb 2497 m
D. NA kt
E. NA deg nm
F. 178 deg 127 kt
G. 90 deg 031 nm
H. EXTRAP 932 mb
I. 11 C/ 3049 m
J. 17 C/ 3049 m
K. 17 C/ NA
L. OPEN SW
M. C33
N. 12345/ 7
O. 0.02 / 1 nm
P. AF300 2212A KATRINA OB 28
MAX FL WIND 127 KT E QUAD 15:06:20 Z
SLP EXTRAP FROM 700 MB
FIX MADE OVERLAND
EYE RAGGED

8. REFERENCES

Black, M. L., H. E. Willgughby, 1992: The Concentric Eyewall Cycle of Hurricane Gilbert. *Mon. Wea. Rev*., **120**, 947-957.

Dodge, P., R. W. Burpee and F. D. Marks Jr.. 1999: The Kinematic Structure of a Hurricane with Sea Level Pressure Less Than 900 mb**.** *Mon. Wea. Rev.,* **127**, 987–1004.

Franklin, J. L. and S. D. Aberson. 1999: Impact on Hurricane Track and Intensity Forecasts of GPS Dropwindsonde Observations from the First-Season Flights of the NOAA Gulfstream-IV Jet Aircraft. *Bull. Amer. Meteor. Soc.,* **80**, 421–427.

Geerts, B., G. M. Heymsfield, L. Tian, J. B. Halverson, A. Guillory, and M. I. Mejia. 2000: Hurricane Georges's Landfall in the Dominican Republic: Detailed Airborne Doppler Radar Imagery. *Bull. Amer. Meteor. Soc.*, **81**, 999–1018.

Goni, G. J. and J. A. Trinanes, 2003: Ocean Thermal Structure Monitoring Could Aid in the Intensity Forecast of Tropical Cyclones. *EOS*, **84**, 573-580.

Gray, W. M. 1968: Global View of the Origin of Tropical Distrubances and Storms. *Mon. Wea. Rev*., **96**, 669-700.

Harasti, P. R., C. J. McAdie, Dodge, P. P., J. Tuttle, S. T. Murillo, and F. D. Marks Jr., 2003: Real-Time Implementation of Single-Doppler Radar Analysis Methods for Tropical Cyclones: Algorithm Improvements and Use with WSR-88D Display Data. *Wea Forecasting,* **19**, 219-239.

Knabb, R. D., J. R. Rhome, and D. P. Brown. 2005: Tropical Cyclone Report: Hurricane Katrina 23-30 August 2005. http://www.nhc.noaa.gov/pdf/TCR-AL122005_Katrina.pdf

Lee, W. C., B. J.-D. Jou, P.-L. Chang, and F. D. Marks Jr.. 2000: Tropical Cyclone Kinematic Structure Retrieved from Single-Doppler Radar Observations. Part III: Evolution and Structures of Typhoon Alex (1987). *Mon. Wea. Rev.,* **128**, 3982–4001.

Lee, W. C. and F. D. Marks Jr.. 2000: Tropical Cyclone Kinematic Structure Retrieved from Single-Doppler Radar Observations. Part II: The GBVTD-Simplex Center Finding Algorithm. *Mon. Wea. Rev*., **128**, 1925–1936.

Marks, F. D., L. K. Shay, and PDT-5, 1998: LandfallingTropical Cyclones: Forecast Problems and Associated Research Opportunities. *Bull. Amer. Meteor. Soc.,* **79**, 305-322.

Powell, M. D., P. P. Dodge, and M. L. Black, 1991: The landfall of Hurricane Hugo in the Carolinas: Surface wind distribution. *Wea. Forecasting*, **6**, 379-399.

Powell, M. D., and S. H. Houston. 1998: Surface Wind Fields of 1995 Hurricanes Erin, Opal, Luis, Marilyn, and Roxanne at Landfall**.** *Mon. Wea. Rev*., **126**, 1259–1273.

Tuttle, J., and R. Gall. 1999: A Single-Radar Technique for Estimating the Winds in Tropical Cyclones**.** *Bull. Amer. Meteor. Soc.,* **80**, 653–668.

Wakimoto, R. M. and P. B. Bloack, 1994: Damage survey of Hurricane Andrew and its relationship to the eyewall. *Bull. Amer. Meteor. Soc*., **75**, 189-200.

Willoughby, H. E., J. A. Clos, and M. G. Shoreibah, 1982: Concentric eyewalls, secondary wind maxima, and the evolution of the hurricane vortex. *J. Atmos. Sci*., **39**, 395-411.